Early View publication on wileyonlinelibrary.com
(issue and page numbers not yet assigned;
citable using Digital Object Identifier – **DOI**)

Ann. Phys. (Berlin), 1–20 (2011) / **DOI** 10.1002/andp.201000139

Historic Article

On an experimentally observed phenomenon on vortex rings during their translational movement in a real liquid

Carl-Heinz Krutzsch

Physical Institute, Technical University, Dresden, Germany

(With 33 figures)

Received 25 March 1939

Translation by

Diogo Bolster[1,*], **Robert Hershberger**[2,**], and **Russell J. Donnelly**[2,***]

[1] Department of Civil Engineering and Geological Sciences, University of Notre Dame, Notre Dame, Indiana 46556, USA

[2] Department of Physics, University of Oregon, Eugene, Oregon 97403-1274, USA

Received 21 October 2010, revised 11 January 2011, accepted 14 January 2011 by U. Eckern
Published online ♣ 2011

Key words Vortex rings, Kelvin waves, instabilities, number of waves.

1 Introduction

In an investigation on vortex rings suggested to me by Prof. Tomaschek, we succeeded in observing a novel phenomenon, namely the appearance of waves on the core of the vortex ring and unstable regions within the rings. The success was mainly attributed to novel coloring method we applied. The present paper presents a thorough description of the observed phenomena, specifically including quantitative observations, and attempts an interpretation of the results.

2 Preceding experiments

The author has published, [1, 2] and a movie about the phenomena was shown at the meeting of the Thuringia-Saxony-Silesia Section of the German Physical Society in June of 1936. There are few papers related to the observations made in this work. P. Czermak [3] writes that he observed oscillations on the periphery and within the continuous sections of vortex rings produced by gun salutes. However, no detailed description is given. A. Indra [4], who produced vortex rings with a smoke box, claims that the vortex rings stop for a brief instant after a certain running time only to continue its movement with more strength afterwards.

* E-mail: diogobolster@gmail.com
** E-mail: robhersh@uoregon.edu
*** Corresponding author E-mail: rjd@uoregon.edu

3 Experimental setup

The experiments presented herein were mostly run in water as for the same initial velocity, motions proceed slower than with air. This makes observations easier.

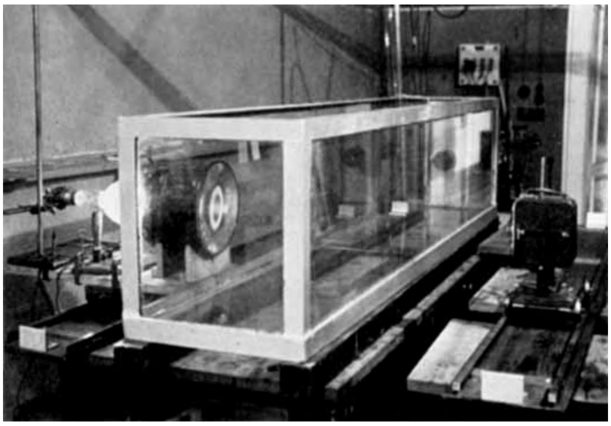

Fig. 1 Water tank with photographic apparatus.

The experimental setup consists of a water trough with internal dimensions $200 \times 40 \times 45$ cm and a tube which is inserted through the center of one of the trough's sides. The trough is open on top and its four sides are made of glass. The side, through which the tube enters, consists of glass and metal (Figs. 1 and 2). Additionally, a second trough with internal dimensions $80 \times 30 \times 35$ cm, which is built in the same manner as the first one, was used. The tube, which enters the trough, is interchangeable. Four different tubes were used in this experiment as shown in Table 1.

Table 1 Internal diameters of piston tubes.

Tube 1	7.6 cm diameter
Tube 2	3.0 cm diameter
Tube 3	2.0 cm diameter
Tube 4	1.5 cm diameter

Inside the tube a piston is installed that ejects water out of the tube. The piston must be as watertight as possible so that no disturbance that occurs before the experiment can affect the dying procedure described below.

In order to assign a precisely defined reproducible impact length and impact velocity to the piston, a control shaft driven by a motor is attached to the piston rod. To measure the piston velocity, a tumbler with graph paper rotates under the forcer rod. A pen on the piston shaft draws the space-time diagram of the forcer's movement. The velocity of the tumbler is held constant by a synchronous motor (Fig. 2).

To record observations and for measurement reasons, photography was deemed necessary. Two directions for exposure were preferentially used: these were perpendicular and parallel to the translation axes of the vortex ring. For exposures perpendicular to the translation axes of the vortex, the photographic apparatus was attached to a cart, which moves alongside the trough on rails. On the other side of the trough, a condenser was also placed on a track. It focused the light of a well-frosted 500 watt bulb through the trough on to the photographic apparatus. The vortex ring was held in the cross hairs in the center of the view finder, which causes the photographic apparatus, the condenser and the lamp all to move with the same velocity as the vortex ring parallel to its translation axes until the most favorable moment for the exposure occurred. This setup guaranteed a high depth of field, as the aperture could be held small with a short exposure time. Most exposures were made with f-stop f/22 and an exposure time of 0.01s. The measurement of the translation velocity of the vortex ring was studied in the same manner by replacing the

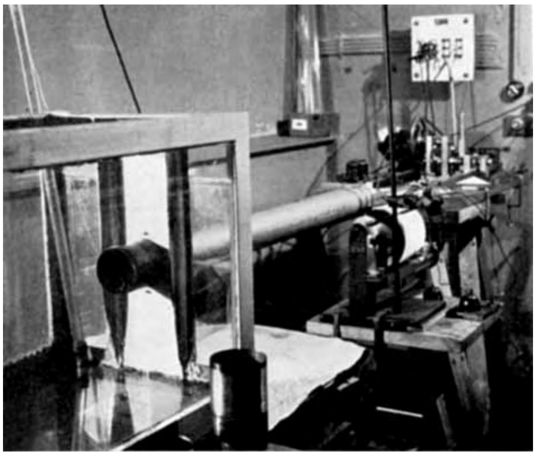

Fig. 2 The gun side of the tank with the motor and piston measurement barrel.

photographic camera with a movie film camera. Inside the trough a leveling rule was installed above the vortices and was also filmed (Fig. 28). To prevent errors caused by the irregular movement of the spring, the camera was coupled to a synchronous motor. The number of pictures per unit time was kept small, 1 picture per 1.5 s, as it became clear this was sufficient to construct adequate time-space curves.

The exposures parallel to the movement direction of the vortex were more complicated. They were examined in a way such that after the production of each vortex ring, a mirror was dropped into the fluid at an angle of 45 degrees. This enabled a side view of the vortex. The track ways with the recording apparatus then approached the trough from the side. We must account for the fact that part of the optical path length, which grows with the movement of the vortex, is in water. The apparatus was therefore moved at 3/4 of the vortex velocity. The light source was located outside the front face of the trough in the direction parallel to the movement axes (see Fig. 3).

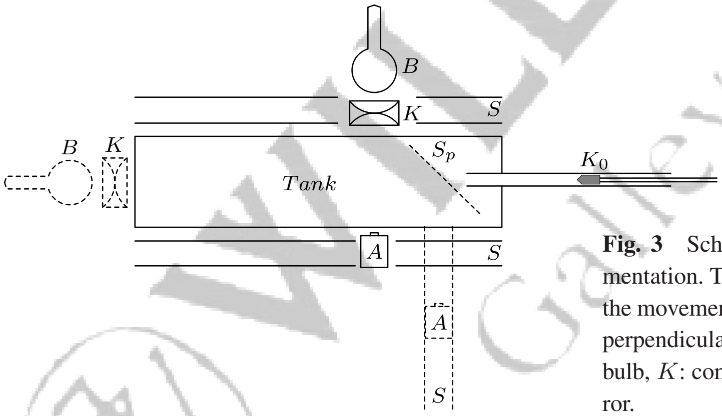

Fig. 3 Schematic alignment for photographic documentation. The dashed lines show exposures parallel to the movement and the solid lines are to show exposures perpendicular to the movement. A: camera, B: 500 W bulb, K: condenser, K_o: piston, S: track way, S_p: mirror.

4 The special dyeing method

To make the vortex visible, a dyeing method was used to either mark a whole or single section of the vortex ring in contrast to the lucent background. Commonly, the whole vortex ring is colored. Thus we dye all of the water contained in the tube. A vortex ring produced in this way has a continuous color distribution over the entire ring. Events taking place within the vortex are not observable with this method.

To observe details within the vortex ring, the coloring method presented here was used. It allows novel insights into the nature of the trajectories of vortex rings. We found that the best method was to apply a

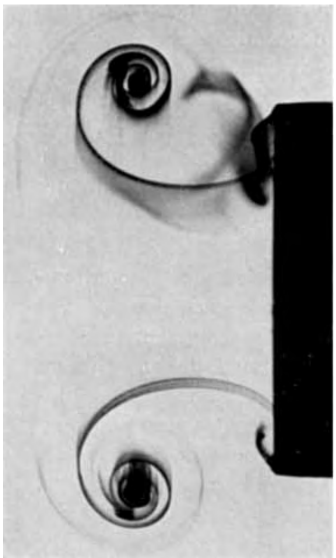

Fig. 4 Formation of a vortex as a cut.

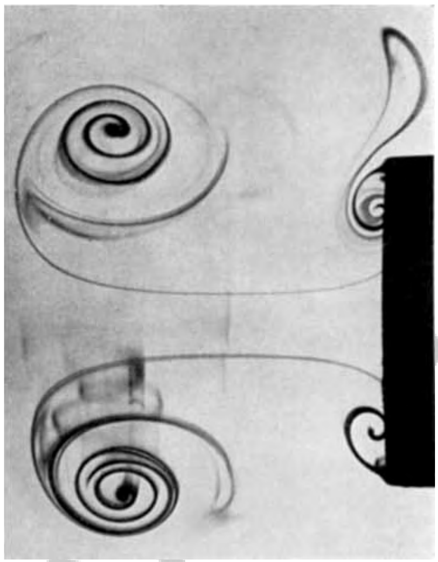

Fig. 5 Formation of a vortex as a cut at a later point of time.

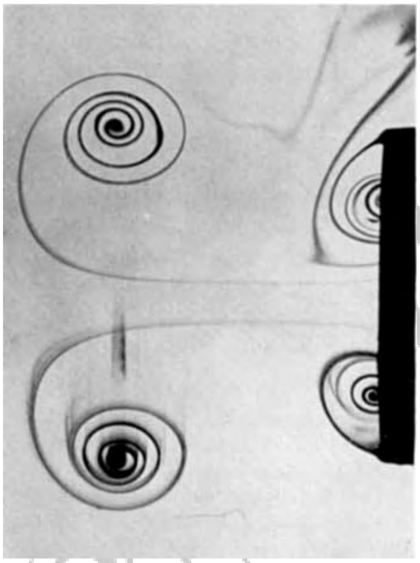

Fig. 6 Formation of a vortex as a cut with a well developed secondary vortex.

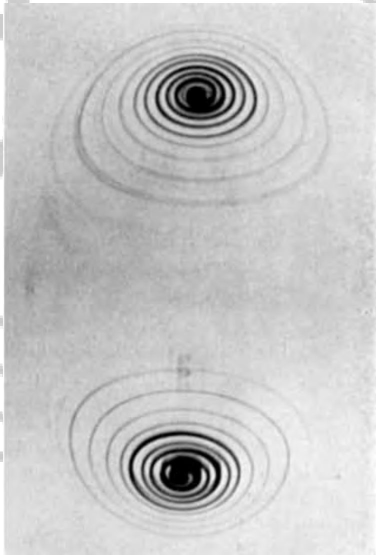

Fig. 7 Normal undisturbed vortex as a cut.

concentrated dye-alcohol solution at the layer of the tube and let it dry. During the impact with the piston some of the dye is dissolved and the vortex core is particularly colored, as the separation layer, which leads to the formation of the vortex ring, formed at the sharply edged exit of the tube. Outer layers show a weaker coloring. It is important to note that the dye is not distributed continuously over the outer layers and that several individual layers can be identified. Looking at a cut through the vortex, the formation and dyeing of

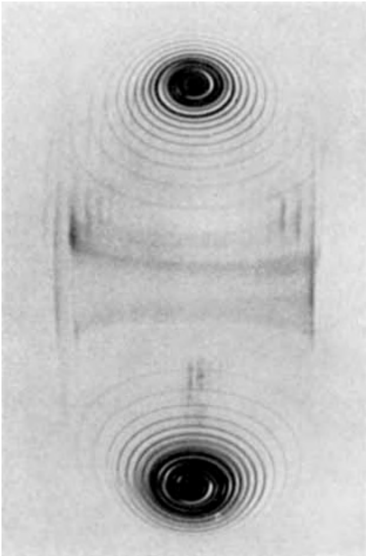

Fig. 8 Normal undisturbed vortex as a cut at a later point in time.

different layers is well observed. In order to obtain a cut through the vortex ring the same method is used. To create a colored cross section, the dye is only applied to the top and bottom of the tube edge, such that the vortex ring remains invisible outside the cross section. As Fig. 4 shows, this leads to the evolution of a dyed spiral with a more strongly colored center. This spiral contracts as shown in Figs. 5 and 6. Also visible in these figures is the evolution of a secondary vortex that is about to travel into the tube. The secondary vortex does not always occur and its evolution depends on the type of impact. The velocity distribution inside the tube is parabolic, and as such this can cause the fluid to stream back along the walls of the tube if the piston movement is decelerated too quickly. Figures 7 and 8 show vortices that have detached themselves from the tube with spirals that are increasingly contracted as the velocity of layers increases towards the center of a vortex.

Different dyes were used, depending on the goal. Sodium fluorescein turned out to be useful. For this dye, the work was done in indirect lighting so as to prevent glare. For the photographic exposures in direct light we could only use a material that either absorbs all colors or only transmits colors for which the chosen film has a minimum sensitivity. For orthochromatic films, a red transmitting fuchsine (magenta) solution was a good choice. For panchromatic films, a malachite-green solution turned out to be useful. The strength of the dye can be varied easily by varying the concentrations.

5 Observations

Observations of a vortex ring during its translational movement, dyed with the method described above, shows that the core of the undisturbed vortex is initially circular. The trajectories of the particles rotating around the core are also circular. After a brief running time a deformation of the outer trajectories is observed. The trajectories change from circular to elliptical paths that are flattened at the center as shown in Figs. 7 and 8. The core of the vortex remains unchanged however. It takes a certain amount of time before also the core of the vortex changes its circular form. Different points on the circle bend towards the vortex center while the parts that remain outside fall back in their translation movement. This process is relatively slow such that it is easily observable for slow vortices. Thus, the core is no longer circular, but surrounds the center like a wave train.

These "Kelvin waves" come in integer quantities, are distributed over the entire vortex ring and can be of an odd or even number. Figures 9 and 10 show vortex rings with Kelvin waves seen from their axis of translation. Figure 11 shows a side view of a vortex ring with Kelvin waves. The number of Kelvin waves depends on the size and velocity of the vortex ring. Kelvin wave numbers from 3 to 15 were observed. We expect that by applying larger velocities, even higher Kelvin wave numbers can be achieved. Figure 12 shows a vortex ring with 12 modes. We note that the amplitude of the waves seems to decrease with an increasing number of waves. Despite the Kelvin waves, the core remains the center of the rotation.

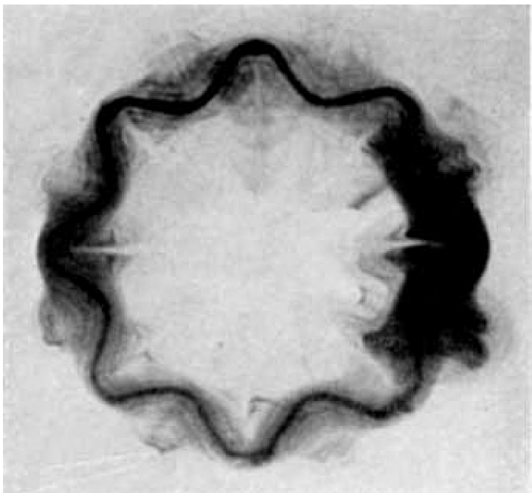

Fig. 9 Vortex ring with eight modes of Kelvin waves.

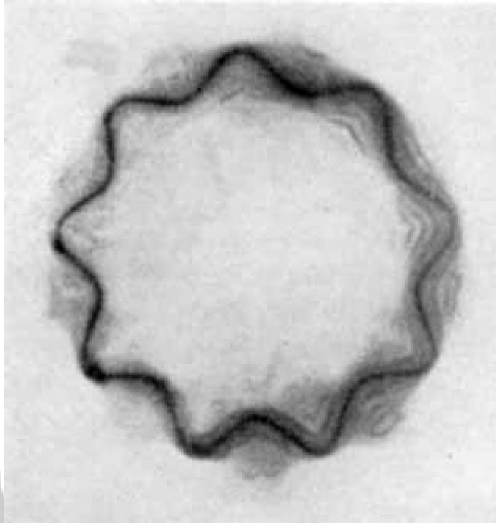

Fig. 10 Vortex ring with nine modes of Kelvin waves.

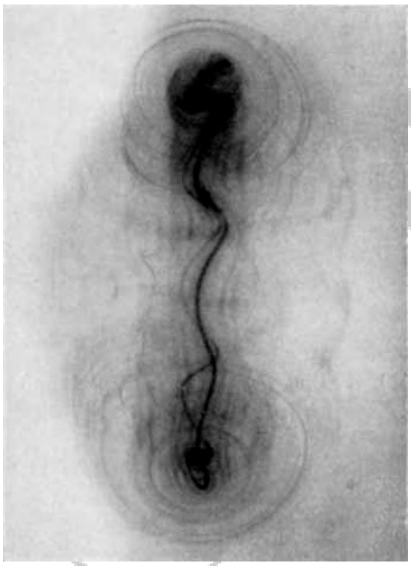

Fig. 11 Vortex ring with waves viewed from the side. Travel is from right to left.

From our observations we note that the emergence of the waves depends on two conditions:

1. The vortex must be undisturbed, i.e. the core must initially be allowed to form an undisturbed circle (e.g. without oscillation) which travels through the surrounding fluid.
2. The rotation velocity of the vortex has to be sufficiently large that the single layers show a clearly observable rotation.

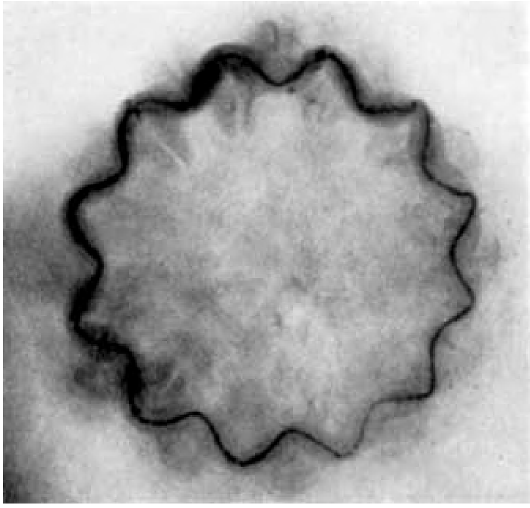

Fig. 12 Vortex ring with 12 modes of Kelvin waves.

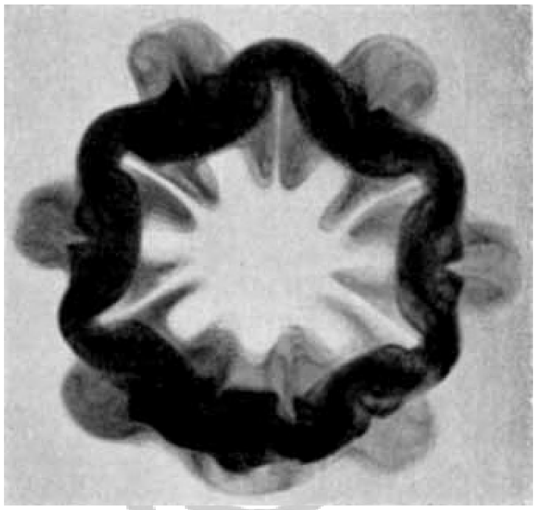

Fig. 13 Relocations in the outer layers in a vortex ring with waves.

Fig. 14 Relocations in the outer layers in a vortex ring with waves.

Therefore, only highly disturbed or slow vortices do not show this behavior.

Continuing the observation of the vortex on its translation path, we observe that the size of the Kelvin waves increases, during which the initially only slightly disturbed outer layers relocate (Figs. 13 and 14). The relocations result in an irregular swirl on one part of the vortex. This irregular swirl, initially just at only one point of the vortex, extends quickly over the whole ring. At this point, the core is no longer the axis of rotation. This instability lasts for a while until the vortex ring quiets down again. After this process, the coloring dye is no longer distributed in only the inner layers, but is spread continuously over the entire vortex ring. During the period of instability, the diameter of the vortex has increased, although the vortex often ejects material into the surrounding area. Highly energetic vortices are less affected by these instabilities than vortices that begin with low energy. For low energy vortices, the instability can result in the complete dissolving of the vortex. Two conditions have to be fulfilled for the instability to occur:

1. The vortex core must have shown the wave formation.
2. The vortex has to be energetic enough for the waves to not degenerate.

The border between the waves and instability is sharp and only smears for ring with a slow rotation.

A second wave instability of the vortex ring is only rarely observed, as the first condition for the appearance of the waves, namely the undisturbed movement of the vortex, cannot be fulfilled a second time, as the first instability causes strong anomaly. Further, any observations of such a second instability are complicated by the fact that the dye is distributed equally over the entire vortex ring now and the different layers are no longer distinguishable.

6 The cause of these events

In order to understand these events one thing is very important: The vortex ring entrains parts of the surrounding medium during the translational motion.

This goes against the models of vortex rings in an ideal fluid or the occasional ideas that treat the ring as being in a real, viscous fluid consisting always of the same set of particles, which assume that any external fluid particles only move to avoid the ring. Hence, the mass of the vortex ring increases steadily. The main contribution to the deceleration of the translational motion is thus not only inner friction but also the transfer of rotational energy to initially motionless masses.

Because this entrainment is essential to the understanding of the observations made earlier the following exploratory experiment was conducted. We aimed to dye the newly entrained fluid. To achieve this we cannot dye all of the exterior fluid as there will be no visible change in color. However, we performed a

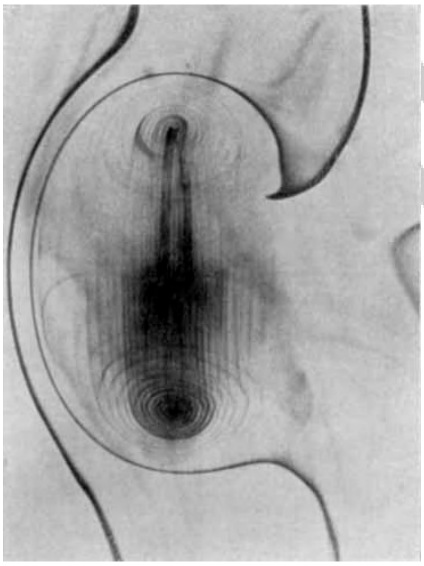

Fig. 15 The rolling in of external fluid into a vortex ring. Travel is from right to left. The ring is passing through stripes of color.

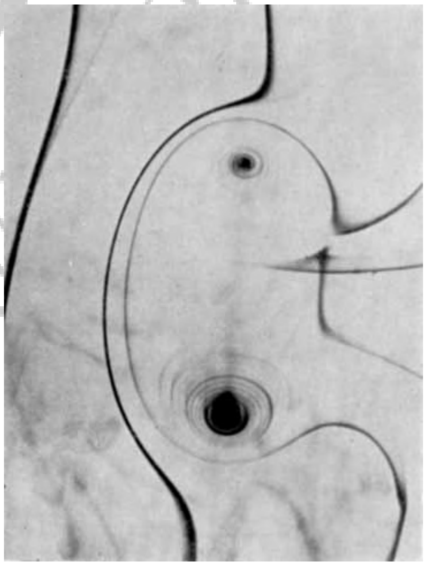

Fig. 16 The rolling in of external fluid into a vortex ring. Travel is from right to left.

dye procedure where dye is only present in a plane perpendicular to the translational axis of motion and is also spaced intermittently. To achieve this we found it best to let dye streams run from the top to the bottom of the tank. For this purpose we placed potassium permanganate crystals at the water surface. The potassium permanganate dissolves and sinks to the floor in colored stripes, since potassium permanganate solution is denser than water. The procedure has to be conducted in still water. If we then send a non-dyed or weakly dyed vortex ring through these color streams, parts of the color streams will be rolled into the ring.

First, the color streams evade the ring, then they attach themselves and finally are roped in from behind. The ring then translates with a newly colored outer layer. Figures 15 and 16 show such a vortex ring.

The entrainment of fluid into the ring gives rise to the question: how does this influence the velocity distribution of single layers and particles within the ring? Assuming that the axial velocities at different distances from the central point of the vortex ring have the distribution shown in Fig. 17 at the beginning of the motion, the velocity distribution will change due to the entrainment of exterior material. If the entrainment is symmetrically distributed across the vortex ring and assuming that the vortex core is only influenced on the whole by the entrainment, this means that the vortex core continues to rotate like a rigid body but with smaller and smaller angular velocities. Then, after some time, a velocity distribution such as that shown in Fig. 18 would occur. However, because of the clash of particles moving in the center of the ring it becomes impossible to entrain matter from this region. The particles therefore only experience a partial deceleration, because the entrainment of external fluid occurs on the outer area of the vortex. Individual particles on a streamline will therefore carry out irregular motions. The velocity distribution would then be given by Fig. 19.

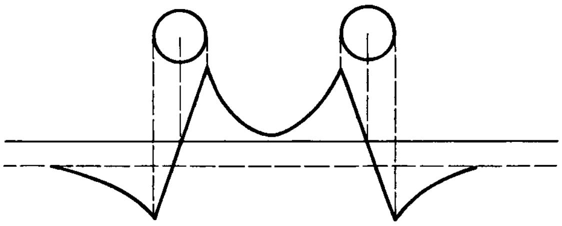

Fig. 17 Assumed axial velocity distribution of the vortex ring.

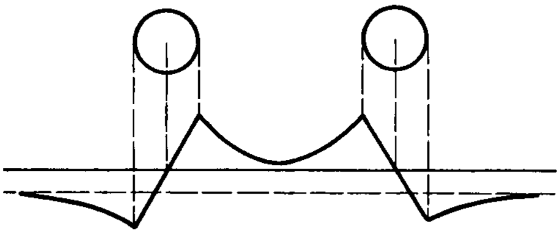

Fig. 18 Axial velocity after some travel by symmetrical influence.

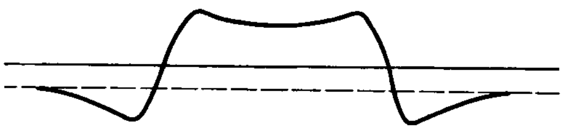

Fig. 19 Axial velocity by asymmetrical influence.

The assumption of this velocity distribution was verified by the following measurements.

Small aluminum particles are inserted into the trough fluid and are lit with an arc lamp through the front side. A slit was placed along the optical path. The light gap, which is parallel to the translational axis of motion, cuts the vortex ring in a plane. By photographing the particles from the side with a longer exposure, lines are revealed in the photograph, which directly correspond to the velocity in that respective area. During exposure the central point of the coordinates was placed in the vortex ring by moving the camera parallel to the translational axis with the velocity of the ring. Figure 20 shows such a photograph that was taken shortly after the formation of the ring. Figure 21 shows a vortex ring that was recorded after a longer running time. Waves had not developed yet.

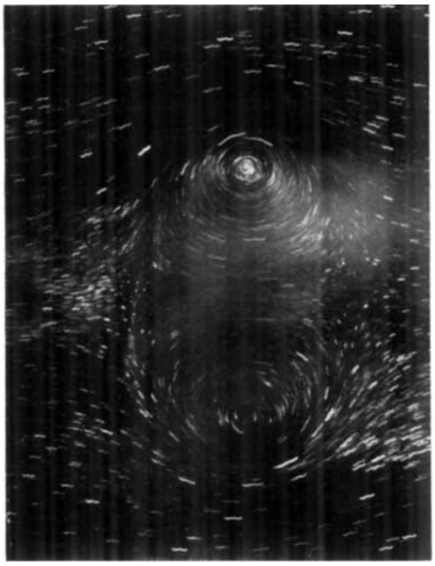

Fig. 20 Photograph of aluminum particles in the vortex ring for determining the velocity distribution. Travel is from right to left.

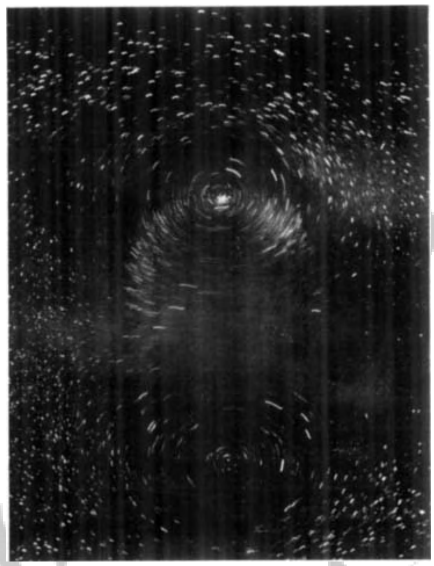

Fig. 21 Same as in Fig. 20 using a longer exposure time.

Figure 20 reveals the axial velocities given in Fig. 22 at different distances from the center of rotation with a cut perpendicular to the rotational axis through the center of rotation. Figure 21 yields the changed velocity distribution shown in Fig. 23, which correspond well with the previously assumed velocity distribution.

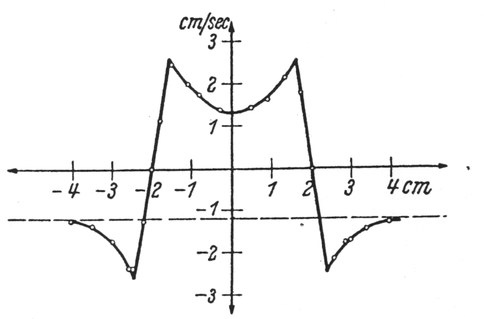

Fig. 22 Axial velocities for different distances with respect to the center after a short running time.

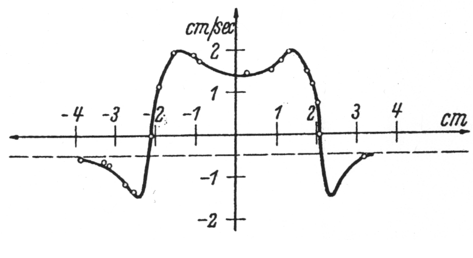

Fig. 23 Axial velocities for different distances with respect to the center after a long running time.

By observing the changes in the velocity distribution of a rotating particle one recognizes that initially the particle moves at almost the same velocity on an orbit around the center of rotation. After some running time the uniform motion will gradually change to a non-uniform motion. The particle will be accelerated on the non-circular orbit in the middle of the ring and will then posses a considerably higher velocity. Outside of the ring the particle will be decelerated. The velocities for one orbit were extracted from Fig. 21 and plotted vectorially (Fig. 24). With this vector diagram it is easy to see the asymmetry of the velocities for one orbit. The particle behaves like it was obtained from the entrainment of liquid.

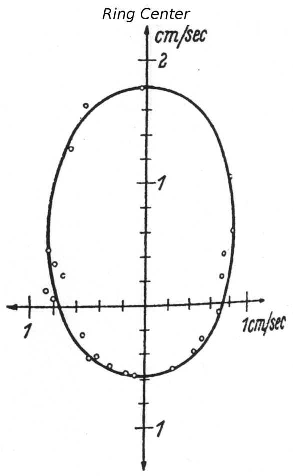

Fig. 24 Vector diagram of the velocities of one orbit with respect to the core of the vortex ring as the origin.

The result of this growing asymmetrical velocity distribution is a growing asymmetrical pressure distribution. An increasing pressure from the outside acts on the slowly moving particles in the vicinity of the core of the vortex ring, which tries to shrink the ring. This overpressure that acts on the core of the vortex ring and the adjacent layers is symmetric around the whole vortex ring and points against itself. By the assumption of continuity the overpressure will cause no changes unless there is a reduction of mass. During translation, the layers that are close to the core of the vortex ring experience a continuously increasing pressure towards the center of the ring due to the continuous deceleration in the outer area and the continuous acceleration in the inner area. The result of this pressure distribution on the ring is the distortion of the circular orbits of the different layers as noted from the photographs in Figs. 7 and 8.

At this moment the core of the vortex ring resides in an unstable balance, which is maintained by the symmetry and the inertia of the rotating masses. If a disturbance occurs at any point on the circumference of the vortex ring, the symmetry of the forces will be perturbed. Such a perturbation would result in a small indentation of the core of the vortex ring. The consequences of this could be many. One must consider the fact that a vortex ring can be thought of as a row of gyroscopes with the same but tilted axes connected via cohesion. If a force is applied to this axis, then a gyroscopic momentum is generated, which is larger the larger the moment of inertia. Thus one small bend of the core of the vortex ring generates a gyroscopic momentum (torque). Since at the distortion the overpressure on the core of the vortex ring increases steadily from the outside to the inside, the bend and the gyroscopic momentum grow. The gyroscopic momentum has the effect that the maximum of the bend is bent in the direction of translation and that the two upper corners of the indentation are pushed in the opposite direction. This rotating motion does not continue because the bend has only a small mobility due to the inertia of the rotating masses further out and the maximum point of the indentation is continually pulled inward. The mobility of the core of the vortex ring and the adjacent layers is lesser the larger the rotational energy of the vortex ring. The bending of the core of the vortex ring forwards and backwards results in a torque at the left and the right of the perturbation whereby two new bends develop on both sides of the first indentation. These two new waves are much weaker if the overpressure from the outside does not support the new perturbations such that the same conditions are reached as for the first bend. During this process the bends/waves do not have to be distributed in an integer number on the circumference. It is easily possible that incomplete waves develop.

These are of short duration for the following reason: In the regions of maximum indentation the pressure from the outside to the inside is amplified because the faster layers in the vicinity of the core come closer to the middle of the ring. A particle that rotates in a layer around the area of maximum indentation will be accelerated in the middle of the ring and decelerated in the outer area. The pressure there will be higher than in the other layers. The opposite happens in the areas of largest bulge. There, the pressure will decrease compared to other layers. With these pressure relations it is easily understood that incomplete waves are eliminated by adjacent indentations. For this reason there will always be an integral number of waves.

The number of waves grows with the velocity and the size of the ring. This observation is explicable by means of this proposed hypothesis: With high rotational energy of the layers close to the core, a small indentation is sufficient to generate a torque, which generates the adjacent waves. Thus a high number of waves will be created on the circumference of the ring.

Similarly, the size of the waves, which decreases with the rising velocity and the size of the ring, depends on the rotational energy of the ring. At a high rotational energy the outer layers are so stable that the core and its adjacent layers have a small mobility. On the other hand the waves and wave number behave oppositely for rings with low energy, which have a small number of waves with larger amplitudes. This corresponds with a later mentioned measurement.

Another occurrence that needs explanation is the phenomenon that causes waves to develop during the translational motion. During flight the vortex ring reduces the number of waves. The cause for that lies in the pressure distribution that was mentioned before. A smaller wave will be absorbed by larger adjacent ones.

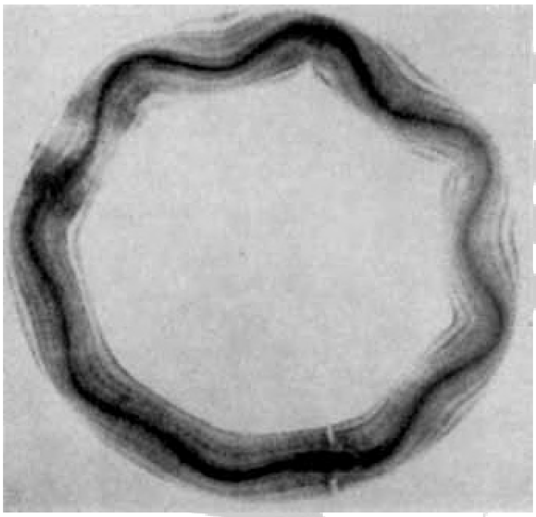

Fig. 25 Vortex ring with waves and a partly undisturbed outer layer.

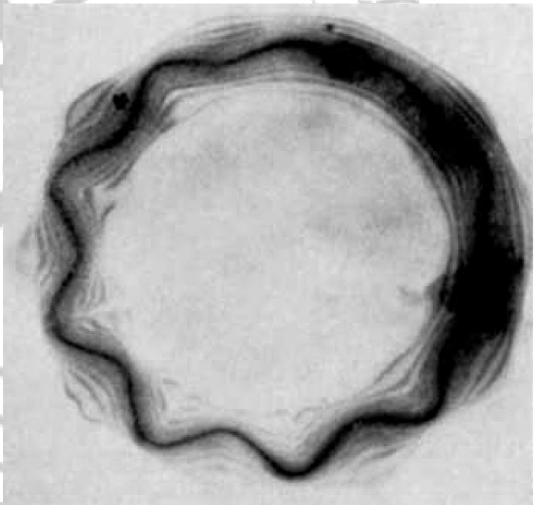

Fig. 26 Vortex ring with waves and a partly undisturbed outer layer.

The onset of the instability determines the increasing torque. As a result of the growing of the wave and the relocation of the layers, the torque becomes so large that it will overcome any counter forces that come from the pressure. When this occurs, the bent center of rotation, namely the core of the ring, rotates around the new axis itself. This double rotation leads then to abnormal vortex rings for which we observe no identifiable laws.

During the previous discussion the origin of the perturbation, which leads to the first wave, was not discussed. Because the vortex ring entrains external fluid at the beginning of its proper motion, as described above, difficulties arise when the vortex ring, due to a lack of space, cannot pick up more matter without

Table 2 Measurement number 1.

Line No.	Stroke Length (cm)	Piston Vel. (cm/s)	R_e	Time to Waves (s)	Time to Instab. (s)	Dist. to Waves (cm)	Dist. to Instab. (cm)	No. of Wave Modes	Ring Dia. (cm)
Tube diameter 7.6 cm									
1	2.13	11.0	3810	12.2	38.2	30.8	75.0	7	5.6
2	3.30	11.4	3880	12.5	31.0	33.5	72.2	8	6.8
3	5.05	10.8	4110	18.5	41.5	50.7	100.2	6	8.2
4	5.70	11.0	3800	14.0	24.0	44.0	93.5	7	8.2
5	8.97	10.9	3770	12.0	18.0	45.0	76.3	9	9.4
6	3.20	13.5	5110	3.0	20.0	7.5	70.0	8	8.8
7	9.33	13.9	5270	9.0	17.0	36.5	73.7	10	9.4
8	4.10	18.9	7180	4.5	15.5	30.0	70.5	10	7.6
9	6.25	18.4	7000	4.0	14.0	30.0	73.0	10	8.8
10	8.08	19.2	7300	5.0	13.0	32.2	80.5	12	9.2
11	2.30	19.1	7250	3.5	13.5	15.0	57.5	8	5.6
Tube diameter 3.0 cm									
12	2.20	10.2	1530	24.0	—	40.5	—	3	3.1
13	5.93	9.7	1460	5.5	13.0	19.0	40.0	6	3.8
14	7.5	9.8	1473	5.0	9.5	18.5	33.6	6	4.0
15	2.95	13.7	2050	11.5	22.0	36.0	57.5	6	3.5
16	7.55	13.8	2075	3.0	6.0	15.3	31.2	6	4.2
17	8.95	13.7	2050	3.0	4.5	17.0	25.0	7	4.3
18	2.15	16.7	2505	7.0	17.0	24.3	48.3	6	4.0
19	4.35	16.5	2470	3.0	6.0	16.0	29.5	8	3.8
20	7.88	16.4	24.62	2.0	3.5	12.0	22.0	—	4.6
21	2.74	21.2	3170	3.0	7.5	14.5	35.5	8	3.5
22	5.40	21.8	3650	1.5	3.0	11.1	22.0	8	4.0
23	7.65	21.2	3170	1.5	4.5	7.3	30.5	8	3.5

increasing its radius. Because an expansion of the radius does not occur owing to the special pressure distribution, a clearance volume will arise behind the ring from where matter will be ejected. This ejection of matter is sufficient to disrupt the unstable equilibrium of the ring and a small indentation is generated. This is the case for an initially undisturbed vortex ring. If the vortex ring has an initially induced perturbation then this is sufficient to generate a wave even earlier. This initial perturbation must not exceed a certain size. Otherwise a wave cannot develop because the velocity distribution and the associated pressure distribution that is necessary for the wave is only able to develop for non-perturbed or slightly perturbed rings.

Table 3 Tube diameter is 7.6 cm.

Line No.	Time to Waves (s)	Time to Instability (s)	Distance to Waves (cm)	Distance to Instab. (cm)	Waves before Instability
Measurement 2 Piston velocity 14.7 cm/s Stroke length 5.2 cm					
1	14.3	26.0	54.0	92.0	10
2	17.2	29.2	63.5	100.5	10
3	14.2	25.0	54.5	94.5	10
4	14.9	25.8	60.5	97.5	10
5	19.8	29.2	71.5	102.0	10
6	12.0	21.2	49.0	83.0	10
7	101.2	22.0	19.5	86.5	10
8	9.9	22.3	44.0	87.0	10
9	14.4	27.2	61.0	102.5	10
10	11.3	20.0	50.0	81.5	10
Measurement 3		Average	55.75	92.7	
Piston velocity 11.4 cm/s Stroke length 2.03 cm					
1	18.2	46.4	44.5	89	7–6
2	14.3	34.5	41.0	76	7–6
3	16.8	41.3	45.0	84	7–6
4	18.8	40.3	47.0	81	6
5	13.8	37.0	38.5	80.5	8–6
6	20.5	46.4	50.0	87.5	6
7	10.9	32.5	34.0	785.5	8–6
8	25.4	61.3	53	96.6	6–5
9	18.2	41.6	46.5	84.2	7–6
10	12.4	32.4	35.	74	7–6
Measurement 4 Piston velocity 9.52 cm/s Stroke length 3.9 cm					
1	24.2	53.6	56.5	101	7
2	26.0	47.4	65.6	103	8–7
3	12.0	37.6	35.0	87	8
4	24.3	49.6	63	104	8–7
5	18.7	45.7	48.5	98	8–7
6	12.2	35.0	35.5	81	9–8
7	25.9	47.1	64.0	99	8–7
8	17.5	48.4	46	103.5	8–7
9	20.4	38.9	47.5	83.5	8–7
10	22.2	51.0	55	104.5	8–6

Table 4 Tube diameter is 7.6 cm, piston velocity is 15.5 cm/s and stroke length is 3.5 cm.

Line No.	Time to Waves (s)	Time to Instability (s)	Distance to Waves (cm)	Distance to Instab. (cm)
Measurement 5				
With perturbation				
1	8.0	14.2	31.0	57.5
2	7.5	13.8	31.5	57.0
3	7.0	14.4	25.5	53.0
4	8.0	14.4	28.0	54.5
5	7.3	13.4	30.5	56.5
		Average	29.3	55.7
Measurement 6				
Without perturbation				
1	14.9	24.1	56.0	82.0
2	10.4	17.3	45.0	67.5
3	14.2	24.2	55.0	84.0
4	11.0	22.0	43.5	74.0
5	18.8	28.4	68.0	92.5
		Average	53.5	80.0

The preceding considerations were motivated through the following experiments:

First, a sequence of photographs of vortex rings was taken that show that the primary event at the origin of the wave is a motion of the core of the vortex ring, as initially the available pressure from the outside to the inside acts only on the core and the directly adjacent layers. Figure 25 shows such a vortex ring that has completely developed waves on one side, while the other side displays only one bend of the core. The outer layers are completely unperturbed in this area. One can observe that the individual layers are influenced less and less by the waves the further out they lie. On the other hand one can observe a relocation of the outer layers for more strongly developed waves. Figure 26 shows another ring with almost unperturbed outer layers. From this picture one can also see that the waves do not evolve in the less perturbed region. Figure 27 shows this more clearly.

From our series of measurements, one can conclude that the evolution of the waves can vary significantly. The evolution of instabilities also varies. This variation is anticipated because the evolution of the waves and the instability depends on a perturbation, which occurs randomly.

The data in Table 2 shows that the fluctuation of the evolution of the wave and the instability depends strongly on the perturbations. In Table 2 line 6 for instance one recognizes that the vortex ring had an initial perturbation by an air bubble in the tube. The fluctuations become clearer when vortex rings are produced with the same initial conditions. For all measurements the length of the stroke of the piston and the velocity of the piston were kept constant.

In measurements 3 and 4 (Table 3) we focus on the number of waves. These decrease as previously described.

For a further examination of the above hypothesis, experiments were conducted that illustrate the behavior of vortex rings with an initial induced perturbation (Table 4). In doing so the following is assumed: The deceleration of the outer particles causes a velocity difference, which leads to an overpressure on the core. By amplifying this deceleration, the wave should occur earlier on average than without a deceleration. The deceleration of the particles on the outer side of the ring was induced by leading an unperturbed

Fig. 27 Partial vortex ring with a non-integer number of waves.

ring through a glass tube with a larger diameter than the ring. The initial formation of the wave and the instability was measured 5 times with a perturbation and 5 times without for a given constant velocity of the piston and constant stroke.

The difference between the measurements with and without the perturbation is significant. The tube section through which the vortex ring moves had a length of only 6.5 cm and was about 10 cm away from the tube opening. The onset of the wave appeared a relatively large distance after passing through the tube section as is seen in the measurements.

It is also possible to induce a wave by an asymmetric perturbation earlier. If the required pressure is high enough, a wave can be produced by touching the ring with a probe during translation. This wave will slowly multiply over the whole circumference of the ring.

7 The translational velocity distribution

As was described at the beginning of the article, photographs were taken to measure the translational velocity distribution. The distance travelled, the onset of Kelvin waves, and the instabilities were measured from the photographs that were taken at intervals of 1.5 seconds (Fig. 28). The plots of distance against time reveal that the translational motion of the vortex ring is described by an exponential function if the ring does not have a perturbation. A logarithmic plot reveals the changes due to the waves and instabilities.

Figures 30 and 29 show the distance-log time-curve of large rings, Figs. 31, 32 and 33 show distance-log time-curve of small rings.

Comparing these curves, one can see that small vortex rings have a completely different behavior than large vortex rings. Large vortex rings show a fluctuation around a straight line, while small rings show a relatively strong bend in the curve. This indicates that two sizes are necessary for the fluctuation around the exponential curve. First, the entrainment process is surely different in the region of waves and instabilities. Second, the ejection of matter out of the ring is much stronger for the smaller rings than for big ones in the regions of instability owing to the smaller stability. This influence may cause the bend in the curve for small rings.

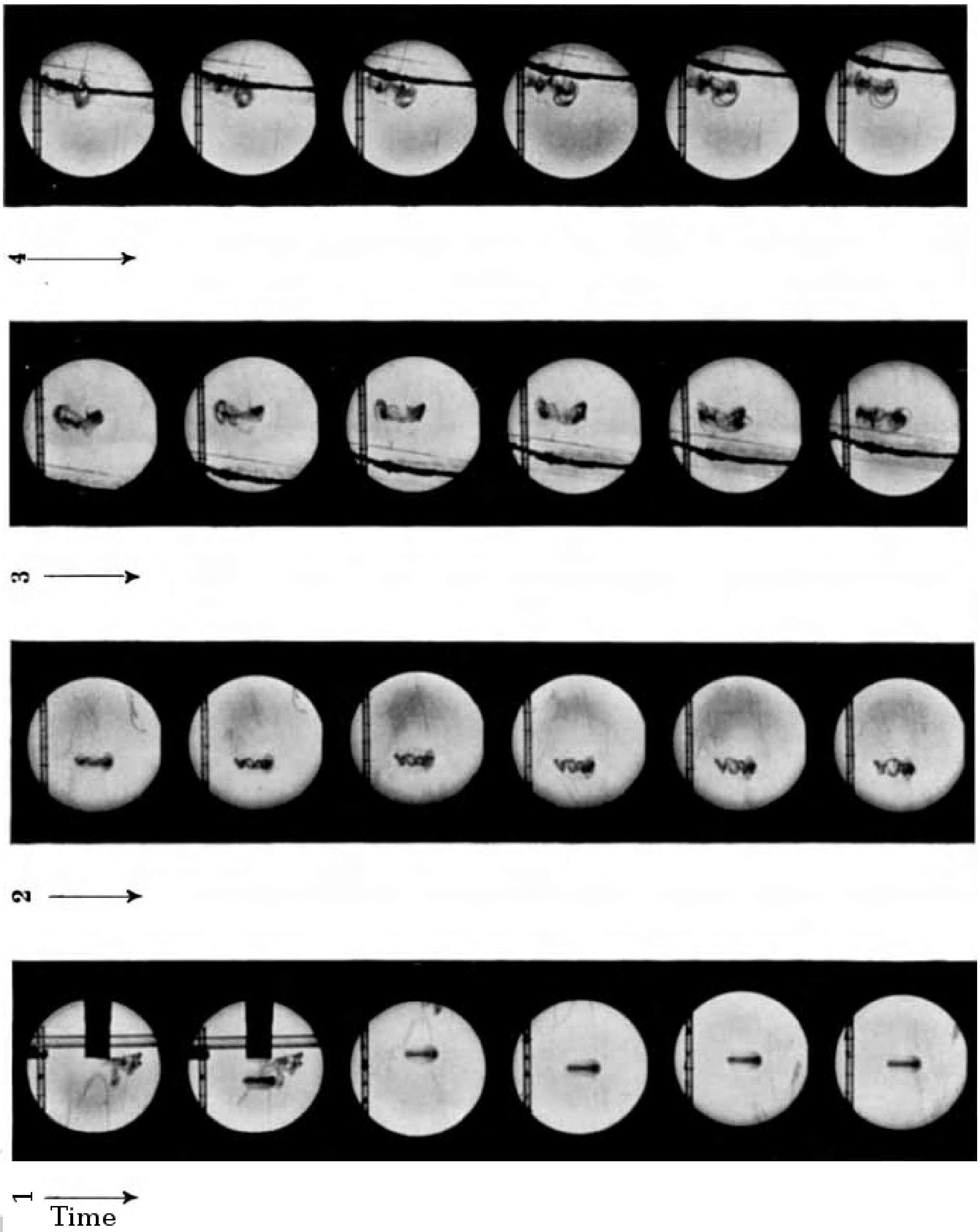

Fig. 28 Filmstrip for the measurement of the velocity distribution. Measurement 1, Table 1, Ring 15. The black line is a caulked crack in the rear glass wall.

8 The influence of viscosity

The experiments conducted so far were all conducted in water, such that it would be of special interest to use fluids of different viscosity.

Experiments in a mixture of glycerin and water, which is 17 times more viscous than water at room temperature, reveal that the waves only appear at higher velocities. At normal velocities such as those used

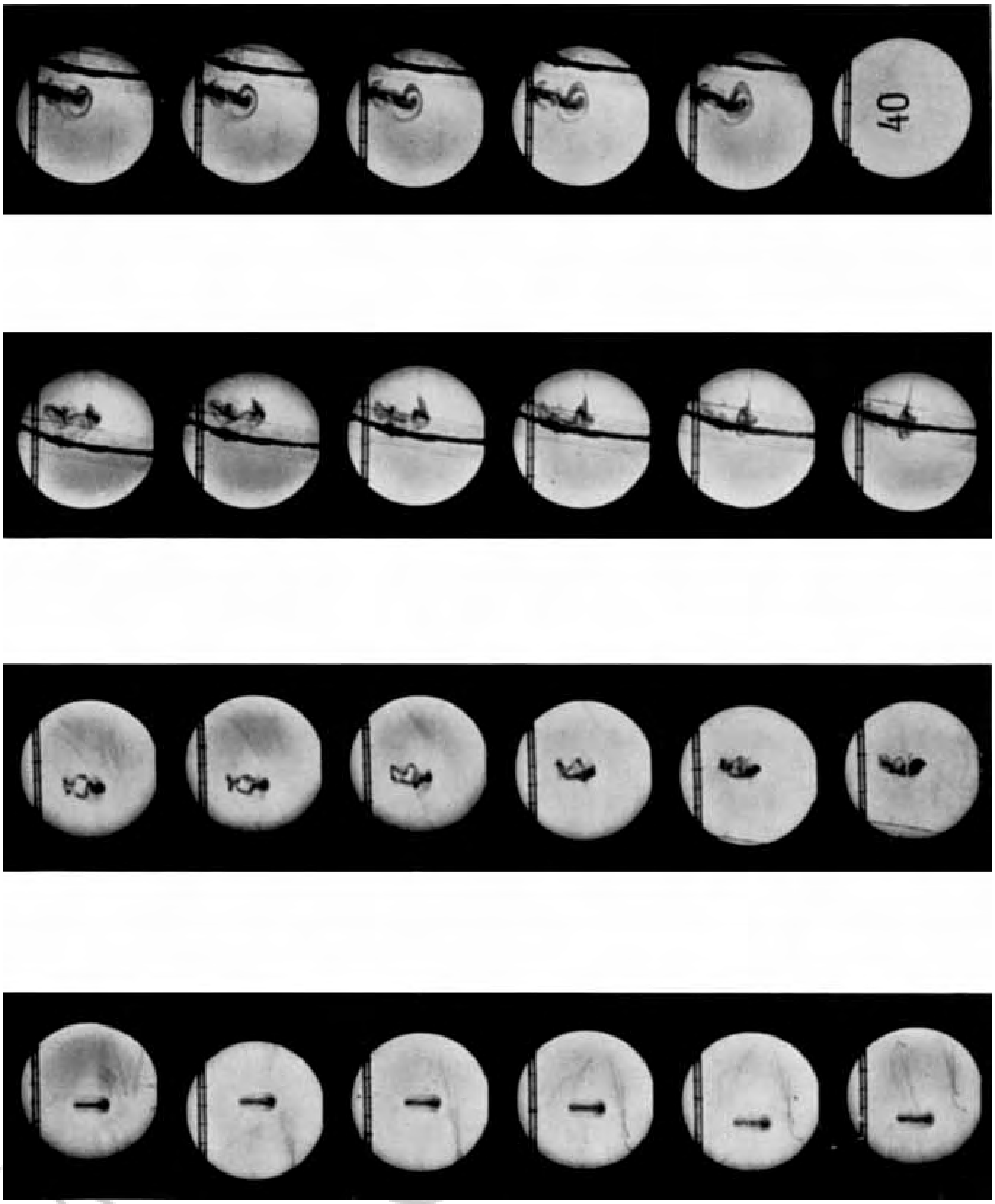

Fig. 28 (Continued.)

in the water experiments, the diameter of the vortex travels without any visible disturbances. Vortices in air, which has 14.5 times the kinematic viscosity of water, do not yield any significantly different observations except for a faster decay of the translational velocity. It is thus not possible to use the Reynolds number for comparison between experiments by simply inserting the translation velocity into it. Even so, the relationship between inertial and viscous forces is the important factor. Thus, instead of the translation velocity, the rotation velocity should be inserted into the Reynolds number. This requires the knowledge of the velocity distribution in the vortex, which will be subject of future investigations.

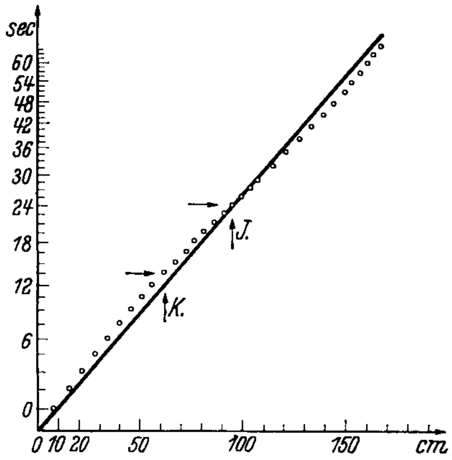

Fig. 29 Distance versus log time of the translational motion of vortex ring number 5 from Table 2.

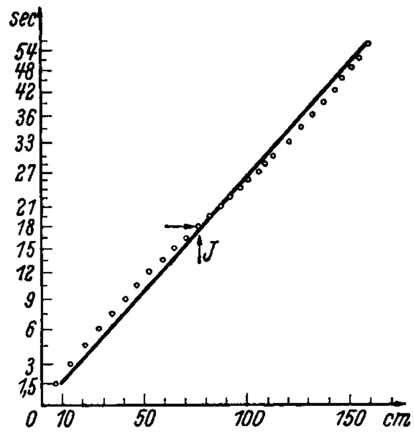

Fig. 30 Distance versus log time of the translational motion of vortex ring number 4 from Table 2.

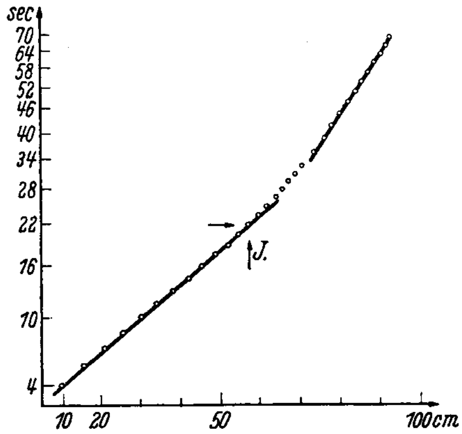

Fig. 31 Distance versus log time of the translational motion of vortex ring number 15 from Table 2.

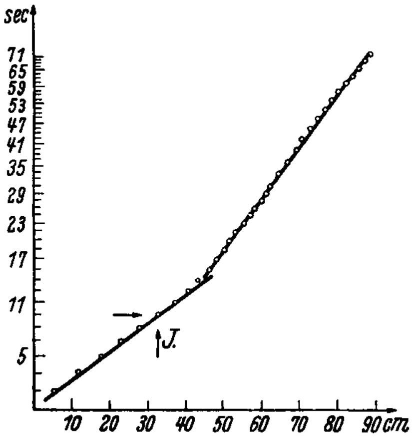

Fig. 32 Distance versus log time of the translational motion of vortex ring number 14 from Table 2.

9 Summary

This paper describes a number of new observations on vortex rings obtained by using a novel dyeing procedure, which has thus far been unknown. Following long investigations, a working hypothesis has been established. It attributes the occurrence of Kelvin waves to the entrainment of external fluid into the ring and a resulting instability, which occurs under the influence of:

1. Friction forces
2. Compression forces
3. Torques

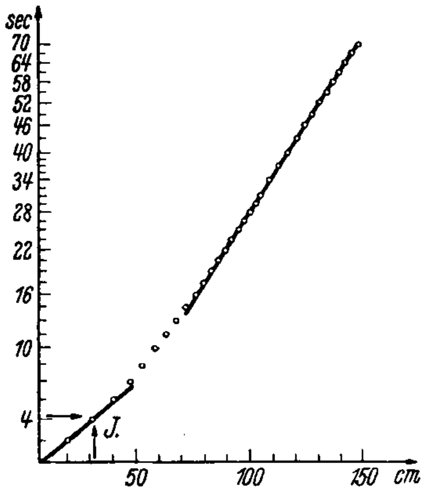

Fig. 33 Distance versus log time of the translational motion of vortex ring number 23 from Table 2.

A continuous evolution of waves within the vortex ring and a resultant instability are caused. The conclusions drawn from this hypothesis are in accordance with all the observations and investigations done so far. A series of different experiments and measurements has made it possible to verify the correctness of the proposed explanation to a large extent.

Acknowledgements As the subject discussed in this paper is mostly virgin soil, some of the observations are only discussed briefly. The purpose of the paper is mostly to describe the problem in general and to bring it to a certain point of clarification. A more detailed analysis and theoretical justification would take much more time and so it seems reasonable to publish the current paper now.

As future work, the measurement of the velocity distribution in the vortex ring up to the point of instability is planned. After the wave formation, the velocity measurement of the different layers does not give the particle's velocity distribution anymore, such that the application of stereo photogrammetry is planned.

I want to thank Prof. Tomaschek for the continual interchange of ideas, his great interest and his invaluable suggestions.

I also want to express my thanks to Prof. Toepler and Dr. Teichman for their innumerable discussions.

Translator's notes and acknowledgements: This paper was published in Berlin in 1939 by an author who has disappeared from the literature of recent years. We think it is less well known than it should be because of the rather formidable technical German in which it was written.

Thanks to Peter Diez and Anika Pflanzer for the original translation and to Chris Hogan for technical assistance. We are grateful also to Professors Jens Noeckel and Dietrich Belitz of the University of Oregon, and to Professor Friedrich Busse of the University of Bayreuth for careful checking of the translation. Finally we are indebted to the Editor for his support in publishing this translation.

References

[1] C. H. Krutzsch, Phys. Zeitschr. **37**, 598 (1936).
[2] C. H. Krutzsch, Z. Angew. Math. Mech. **16**, 352 (1936).
[3] P. Czermak, Wiener Berichte **109 IIa**, 878 (1900).
[4] A. Indra, Wiener Berichte **110 IIa**, 335 (1901).